Non-equilibrium transport through a vertical quantum dot in the absence of spin-flip energy relaxation

T. Fujisawa[1],* D. G. Austing[1],† Y. Tokura[1], Y. Hirayama[1,2], and S. Tarucha[1,3,4]
[1]*NTT Basic Research Laboratories, NTT Corporation, 3-1 Morinosato-Wakamiya, Atsugi, 243-0198, Japan*
[2]*CREST, 4-1-8 Honmachi, Kawaguchi, 331-0012, Japan*
[3]*University of Tokyo, Bunkyo-ku, Tokyo, 113-0033, Japan and*
[4]*ERATO Mesoscopic Correlation Project, 3-1, Morinosato-Wakamiya, Atsugi, 243-0198, Japan*

We investigate non-equilibrium transport in the absence of spin-flip energy relaxation in a few-electron quantum dot artificial atom. Novel non-equilibrium tunneling processes involving high-spin states which cannot be excited from the ground state because of spin-blockade, and other processes involving more than two charge states are observed. These processes cannot be explained by orthodox Coulomb blockade theory. The absence of effective spin relaxation induces considerable fluctuation of the spin, charge, and total energy of the quantum dot. Although these features are revealed clearly by pulse excitation measurements, they are also observed in conventional dc current characteristics of quantum dots.

A quantum dot (QD) is a small conducting island in which electrons occupy discrete energy states [1]. Energy relaxation from an excited state (ES) to a ground state (GS) inside a QD is significantly suppressed if a spin flip is required [2, 3, 4]. Our measurements on QDs in the Coulomb blockade (CB) regime indicate an extremely long spin-flip energy relaxation time, $\tau_{spin} > 1$ μs [4, 5], which is much longer than the interval of tunneling events (Γ^{-1} = 1 - 100 ns for a typical tunneling current of 1 - 100 pA, where Γ is the tunneling rate) as well as the momentum relaxation time, $\tau_{mo} \sim 1$ ns [6, 7, 8]. In the absence of efficient energy relaxation, excess energy remains in the system. This opens up novel non-equilibrium transport channels, which we describe in this Letter.

We start from the orthodox theory which describes CB and single electron tunneling (SET). The total energy, $U(N)$, of the system, in which an island containing N electrons is affected by a gate voltage, V_g, via a capacitance, C_g, is

$$U(N) = \frac{(-Ne + C_g V_g + q_0)^2}{2C_\Sigma} + E_{int}(N) \qquad (1)$$

[1, 9]. The first term is the electrostatic energy approximated by a constant Coulomb interaction. Inside the parenthesis is the sum of the charge on the dot, the induced charge by the gate, and an offset charge, q_0. C_Σ is the total capacitance of the dot. The second term, $E_{int}(N)$, is the sum of the energies of the occupied N electron levels, measured relative to the Fermi energy of the leads, accounting for the internal degrees of freedom of the QD. Other corrections to many-body interactions are also included in E_{int}. In the orthodox theory, originally considered for a continuum density of dot states, the second term is neglected because *the QD is assumed to relax quickly to the minimum energy, $E_{int}^{(\min)}$, which is independent of N*. In this SET scheme, an electron that has entered the island leaves before another electron is allowed to enter when $U(N_0) = U(N_0 + 1)$ as shown in Fig. 1(a). This situation is maintained unless the excitation energy exceeds the charging energy, $E_c \equiv e^2/C_\Sigma$. In this picture spin is neglected and N-electron GSs are only considered.

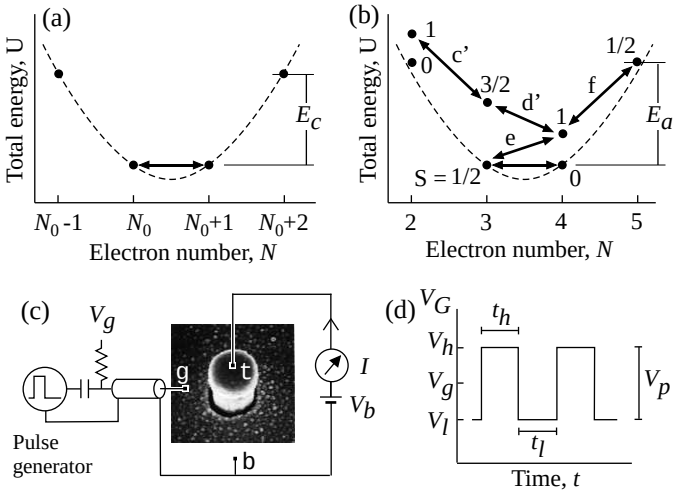

FIG. 1: (a) Total energy $U(N)$ of a small classical island when SET allows N to fluctuate between N_0 and $N_0 + 1$. (b) $U(N, S)$ of QD-1 at B = 3 T and $V_G \sim$ -1.7 V. The arrows indicate allowed tunneling transitions with excitation energy $< E_a$ (see text). (c) Schematic setup for the pulse measurement on a vertical QD. The circular pillar is of diameter 0.54 μm (0.50 μm) for QD-1 (QD-2). See Ref. [12] for details. All the measurements are performed at a temperature $\lesssim$ 0.1 K. The magnetic field is applied parallel to the current. (d) The time-dependent gate voltage $V_G(t)$.

For a QD in which energy quantization and many-body interactions are significant, we must consider the discrete energy of the dot, $E_{int}(N, S, M)$, which is characterized by total spin, S, and total angular momentum, M [1]. We focus on the regime $\tau_{spin} \gg \Gamma^{-1} \gg \tau_{mo}$, where spin-flip energy relaxation is effectively absent. This is the

typical condition for a dot weakly coupled to the leads – the coupling to the leads is still strong enough to give a measurable current ($e\Gamma > 1$ fA), but weak enough to prevent cotunneling current. *If the QD is excited to any N-electron state with a different total spin from that of the N-electron GS, the ES cannot always relax to the GS before the QD undergoes a tunneling transition to another $N \pm 1$ electron state.* Successive tunneling transitions force the QD into highly nonequilibrium configurations. Nonetheless, there is always a selection rule for the tunneling transition to be satisfied: each tunneling transition changes N by one and S by one half. Tunneling transitions which change S by more than one half should be blocked (spin blockade) [10, 11]. Figure 1(b) shows a particular $U(N, S)$ diagram, which can actually be realized in our QD (see below). Long lived ESs are now included, and the different spin states have different energies because of direct Coulomb and exchange interactions[12, 13, 14]. The allowed tunneling transitions indicated by the arrows require an excitation energy smaller than the addition energy, E_a. All these transitions can cause the dot state (N, S, and U) to fluctuate dramatically.

In order to investigate highly non-equilibrium transport, we employ a pulse excitation technique [4], *which generates only transient current associated with long-lived spin states*, on two vertical QDs (QD-1 and QD-2) [12, 13, 14]. Electrons are confined laterally by an approximate two-dimensional harmonic potential (confinement energy $\hbar\omega_0 \sim 4$ meV for QD-1 and ~ 2.5 meV for QD-2). These samples show qualitatively the same behavior. The N-dependent addition energy, $E_a = 2$ - 5 meV, of QD-1 clearly reveals a shell structure [12]. N, S and M can be identified from the magnetic field, B, dependence of the SET current spectrum. Zeeman splitting is not resolved so we neglected it. A square pulse of amplitude V_p, combined with the static gate voltage, V_g, is applied to the gate electrode (g) shown in Fig. 1 (c) [4]. The time dependent gate voltage, $V_G(t)$, illustrated in Fig. 1(d), is $V_G = V_h \equiv V_g + \frac{1}{2}V_p$ during the high phase of the pulse, and $V_G = V_l \equiv V_g - \frac{1}{2}V_p$ during the low phase. A small dc bias voltage $V_b = 0.15$ mV is applied so that electrons are injected from the bottom contact b ($\Gamma_b^{-1} \sim 10$ ns), and escape to the top contact t ($\Gamma_t^{-1} \sim 100$ ns). The averaged dc current, I, is measured during the V_G-pulse irradiation.

Figures 2(a) and (b) show pulse excited current spectra of QD-1 for $N = 0$ - 5 at $B = 3$ T. A current peak initially observed in the absence of the V_G-pulse is always split into two peaks of equal height, when the V_G-pulse is applied. Weaker additional peaks indicated by the arrows are due to transient current through ESs [4]. The pulse length ($t_h = t_l = 300$ ns) is chosen to be much longer than τ_{mo}, but much shorter than τ_{spin}. In this case, transient current through an N-electron ES is only observed when the ES has a total spin different from that of any other lower lying N-electron state [4, 5].

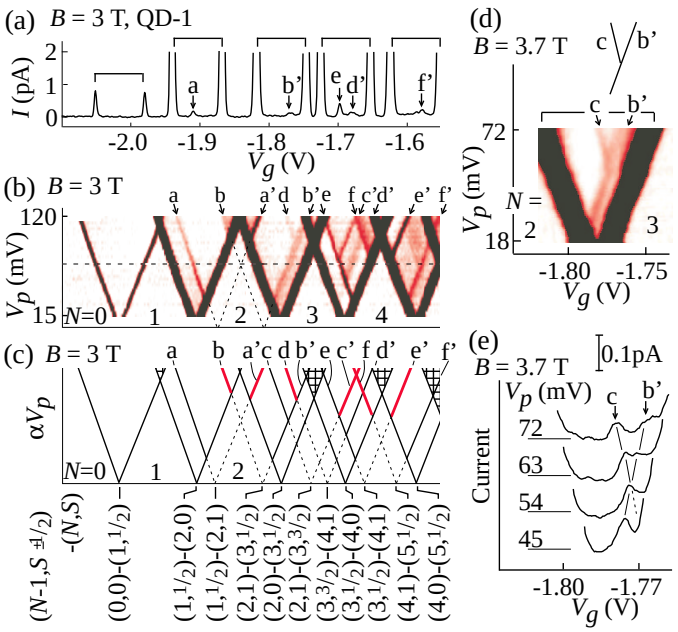

FIG. 2: (color). (a) Pulse excited current I vs. gate voltage, V_g, for QD-1 measured at $B = 3$ T and $V_p \sim 80$ mV [dashed line in (b)]. Each horizontal bar indicates the V_g region where N can fluctuate. (b) Pulse excited current plot at $B = 3$ T built up from I vs. V_g. The color represents current amplitude [white (0 pA) - red (0.25 pA) - black (≥ 0.5 pA)]. N is fixed in each triangular region along the bottom due to CB. (c) Representation of current peaks (solid lines) observed in (b). The transient current peaks are marked by a, a′, b, b′, etc. The prime (non-prime) indicates transport during the low (high) phase of the pulse. These peaks are extrapolated to $V_p = 0$ V as shown by dashed lines. The tunneling transitions between $(N-1, S \pm \frac{1}{2})$ and (N, S) states are also given. The red lines indicate current peaks attributed to the novel DET process, while cross-hatched regions indicate where normal DET occurs. (d) Pulse excited current plot [white (0 pA) - red (0.15 pA) - black (≥ 0.3 pA)] between $N = 2$ and 3 at $B = 3.7$ T. The inset schematically shows the termination of line c by line b′. (e) The I vs. V_g data at various V_p values. The curves are offset for clarity.

Examples of transient current excited by the V_G-pulse for $N = 1$, 2, and 3, are depicted in Fig. 3(a) (c) and (e), where $U(N, S)$ is plotted against V_G. The normal GS-GS tunneling current peaks occur at level crossings labeled ○, whilst transient current appearing at higher energy level crossings are denoted by different symbols. Figure 3(a) shows U for $N = 1$ and 2, where a GS-ES tunneling transition labeled • takes place. Consider that a V_G-pulse is applied as indicated. Suppose the system is in the GS $(N, S) = (1, \frac{1}{2})$ during the low-phase of the pulse ($V_G = V_l$). When the high-phase of the pulse is applied ($V_G = V_h$), the system changes non-adiabatically from $(1, \frac{1}{2})$ at $V_G = V_l$ to $(1, \frac{1}{2})$ at $V_G = V_h$ (indicated by arrow i), since the rise time of the V_G-pulse (1 - 2 ns) is shorter than Γ_{tot}^{-1} ($\Gamma_{tot} = \Gamma_t + \Gamma_b$). If V_h is tuned so that $U(1, \frac{1}{2}) =$

$U(2,1)$, transient current can flow at the crossing marked •. Only a few electrons can tunnel through the ES$(2,1)$, before the inelastic tunneling transition changes the state from $(1,\frac{1}{2})$ to $(2,0)$ [4]. This transient current appears if the pulse excitation energy, αV_p, exceeds the level spacing $\Delta_2 \equiv U(2,1)-U(2,0)$ as indicated, where $\alpha \equiv d[U(N)-U(N-1)]/dV_G$ is the conversion factor from gate voltage to energy. The condition for the transient current to flow is given by the thick line marked • in the αV_p - V_g plane of Fig. 3(b). This current is clearly seen as peak a in Fig. 2(b) [15].

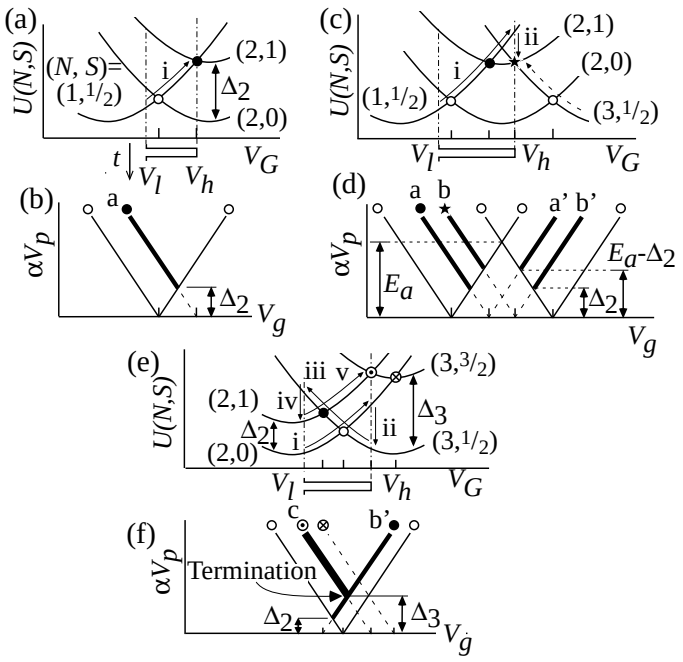

FIG. 3: (a), (c), and (e): The gate voltage, $V_G(t)$, dependence of the total energy. The electron number N and total spin S are indicated by (N,S). The arrows indicate the excitation/relaxation processes discussed in the text. The symbols indicate transport processes (∘ for GS-GS tunneling, • for GS-ES tunneling, ⊗ for spin-blockade, ⊙ for ES-ES tunneling, and ⋆ for novel DET). (b), (d), and (f): Corresponding conditions for stable GS-GS tunneling current (thin lines) and transient current (thick lines). The horizontal axis is the static gate voltage, V_g, while the vertical axis is the excitation energy of the V_G-pulse ($=\alpha V_p$).

Next, we consider striking features for which the conventional SET scheme collapses. Consider the $U(N,S)$ for the $N=1$, 2, and 3 states in Fig. 3(c). Suppose a V_G-pulse, $\alpha V_p < E_a$, is applied as shown. If the state is initially $(1,\frac{1}{2})$ at $V_G = V_l$, $U(1,\frac{1}{2})$ is raised to a higher energy at $V_G = V_h$ (arrow i), and subsequent inelastic tunneling results in either the $(2,0)$ or $(2,1)$ state. If it is $(2,1)$ (arrow ii), it is now possible for another electron to be transported at the crossing $U(2,1) = U(3,\frac{1}{2})$ marked by ⋆. In this case transient transport persists until the inelastic tunneling transition from $(3,\frac{1}{2})$ to $(2,0)$ occurs, because spin-flip energy relaxation from $(2,1)$ to $(2,0)$ is absent. The QD returns back to the initial state $(1,\frac{1}{2})$ when the pulse is switched to V_l. This new tunneling process involves three charge states, and thus we consider it to be novel double electron tunneling (DET). Conventional DET within the orthodox CB theory appears only for $\alpha V_p \geq E_a$ [1, 9], while the novel DET takes place even for $\alpha V_p < E_a$. This process should appear on the thick line b in the αV_p - V_g plane of Fig. 3(d).

The novel DET is clearly seen in the experimental data of Fig. 2(b) as marked by b. Note that this peak cannot be due to regular SET involving higher lying $N=2$ ESs. The spin singlet ($N=2$ GS at $B=3$ T) and the spin triplet [peak a in Fig. 2(b)] are the only possible spin configurations. So no other ESs with different total spin can appear in the pulse measurement. Therefore, the pulse measurement successfully allows us to identify the extra peak b as a novel DET feature. Note that we can also confirm that peak b is due to novel DET from the B-dependence of the peak position [16].

Transient current can also appear during the low phase of the pulse. If a pulse is applied to excite the QD along $(3,\frac{1}{2})$ in the direction of decreasing V_G [dashed arrow in Fig. 3(c)], GS-ES tunneling between $(3,\frac{1}{2})$ and $(2,1)$ should appear along line b′ in Fig. 3(d). Similarly, novel DET appears at the crossing $U(2,1) = U(1,\frac{1}{2})$ [corresponding to feature a′ in Fig. 3(d)]. Note that the extrapolated lines a and a′ (b and b′) meet at zero excitation energy. These features are clearly seen in Fig. 2(b).

We now discuss spin-blockade and associated non-equilibrium transport. Figure 3(e) is the energy diagram for $N=2$ and 3 – the first case where spin-blockade appears. The direct transition between the GS $(2,0)$ and ES $(3,\frac{3}{2})$ is spin-blockaded (marked ⊗). However, non-equilibrium tunneling between the ES $(2,1)$ and ES $(3,\frac{3}{2})$ (marked ⊙) is allowed if a pulse is applied as indicated. Even though the QD is initially in the GS $(2,0)$ at $V_G = V_l$, it first changes to $(3,\frac{1}{2})$ at $V_G = V_h$ (arrows i and ii), then to either $(2,1)$ or $(2,0)$ during the next low-phase [arrows iii and iv for $(2,1)$]. If it is $(2,1)$, ES-ES tunneling occurs at $U(3,\frac{3}{2}) = U(2,1)$ when the high-phase is restored (arrow v). This kind of tunneling mechanism leads to the fluctuation of the total spin from 0 to $\frac{3}{2}$. Note again that this non-equilibrium fluctuation is attributed to the absence of effective spin relaxation. This ES-ES tunneling process requires complex excitation. The excitation energy must be greater than the corresponding two level spacings: $\alpha V_p > \Delta_2 \equiv U(2,1) - U(2,0)$ for the excitation indicated by arrow iii, and $\alpha V_p > \Delta_3 \equiv U(3,\frac{3}{2}) - U(3,\frac{1}{2})$ for the excitation indicated by arrow v. The condition for ES-ES tunneling is marked by line c (⊙) in Fig. 3(f). This line is terminated by line b′ (•) for GS-ES tunneling at $V_G = V_l$, so line c does not reach the line ∘ for GS-GS tunneling. This termination is the signature of an ES-ES

tunneling process which does not involve any GS.

We can identify these features in our QD. Peak c in Fig. 2(d) and (e) now measured at $B = 3.7$ T is attributed to ES$(2,1)$ - ES$(3,\frac{3}{2})$ tunneling from the B-field dependence of the peak position. This peak is clearly terminated by peak b′, which is similarly assigned to ES$(2,1)$ - GS$(3,\frac{1}{2})$ tunneling. However, no measurable current (< 10 fA) is seen for spin-blockaded tunneling between $(2,0)$ and $(3,\frac{3}{2})$ in the region $V_p = 50$ - 100 mV and $B = 3.5$ - 4.1 T (not shown) where spin blockade is expected. These observation are consistent with the above explanation. Note peak c is too weak to see at $B = 3$ T [Fig. 2(b)]. Nonetheless, the following are very clear in Fig. 2(b) for $N = 3$ and 4: ES $(3,\frac{3}{2})$ - ES $(4,1)$ tunneling line d′ is terminated by GS $(3,\frac{1}{2})$ - ES $(4,1)$ tunneling line e, and the termination is associated with spin-blockaded ES$(3,\frac{3}{2})$ - GS$(4,0)$ tunneling (no signal).

Other complicated tunneling processes involving both novel DET and ES-ES tunneling are observed. Peak d (c′) in Fig. 2(b), which is terminated by peak b′ (e), is assigned to ES-ES tunneling, whose excitation process involves three charge states. The observed pairs of tunneling lines (c - c′, d - d′, etc.) always coincide when extrapolated to $V_p \sim 0$ V. More complicated excitations are expected for many-electron QDs. Four different peaks [e, f, c′ and d′ in Fig. 2(b)] are observed between the $N = 3$ and 4 CB regions. The corresponding transitions are indicated in the total energy diagram in Fig. 1(b). The fluctuation in the total energy can be significantly greater than αV_p. Non-equilibrium transport can lead to the accumulation of energy in excess of the excitation energy. As N increases, many long-lived ESs with different S can contribute to the transport. The complexity of many-body excitations increases with αV_p and N [17].

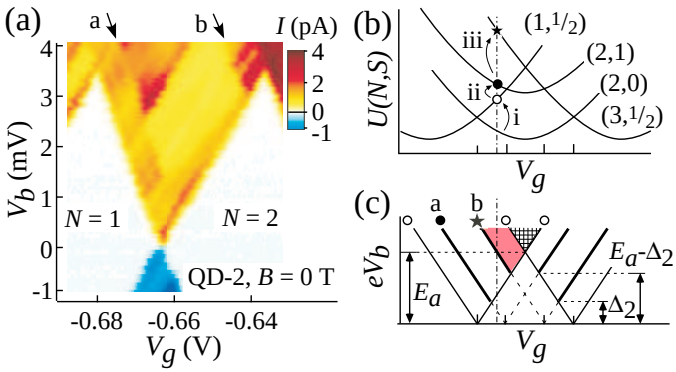

FIG. 4: (color). (a) Color plot of the dc current I in the V_b - V_g plane of QD-2 at $B = 0$ T. The current increases stepwise along the line marked by arrows a and b, which are assigned to normal GS-ES tunneling and the novel DET, respectively. (b) Total energy $U(N,S)$ for the dc excitation processes. (c) Corresponding conditions for the dc excitation transport in the eV_b - V_g plane. Novel DET appears in the red region.

Although our findings till now are deduced from pulse measurements, we expect to see related features in conventional dc excitation measurements. For example [see Fig. 4(b)], novel DET involving $N = 1$, 2, and 3 is allowed in dc measurements when eV_b is greater than $|U(1,\frac{1}{2}) - U(2,0)|$ (energy required for normal SET between $N = 1$ and 2 GSs, arrow i), $|U(2,1) - U(1,\frac{1}{2})|$ (excitation energy to the $N = 2$ spin-triplet ES from the $N = 1$ GS, arrow ii), and $|U(3,\frac{1}{2}) - U(2,1)|$ (extra energy for novel DET, arrow iii). The necessary conditions for the novel DET are satisfied in the red region in the eV_b-V_g plain of Fig. 4(c). Note that this complex excitation can only occur if $\tau_{spin} \gtrsim \Gamma^{-1}$. Figure 4(a) shows the tunneling current spectrum of QD-2 between $N = 1$ and 2 CB regions at $B = 0$ T with no V_G-pulse. In addition to the expected current step marked by arrow a associated with excitation to the ES$(2,1)$, we see an extra current step marked by arrow b associated with the novel DET [18]. Note that the condition in dc measurement for novel DET as well as the other tunneling processes is equivalent to that in pulse measurements, by taking αV_p equivalent to eV_b.

In summary, we have discussed novel DET, which can lead to considerable charge fluctuation, and ES-ES tunneling, which gives rise to significant fluctuation in the total spin. These non-equilibrium transport processes cannot be explained by orthodox Coulomb blockade theory, and arise from the absence of effective spin relaxation inside a quantum dot. With miniaturization of semiconductor devices selection rules for tunneling transitions have to be considered when manipulating spin and charge in a quantum dot.

* Electronic address:fujisawa@will.brl.ntt.co.jp.
† Present address:National Research Council of Canada. Ottawa, Ontario K1A 0R6, Canada.

[1] L. P. Kouwenhoven *et al.*, Reports on Progress in Physics **64**, 701 (2001).
[2] A. V. Khaetskii and Yu. V. Nazarov, Phys. Rev. B **61**, 12639 (2000).
[3] M. Paillard, *et al.*, Phys. Rev. Lett. **86**, 1634 (2001).
[4] T. Fujisawa, Y. Tokura, and Y. Hirayama, Phys. Rev. B **63**, 081304(R) (2001), Physica B **298**, 573 (2001).
[5] T. Fujisawa *et al.*, to be published in Physica B.
[6] U. Bockelmann, Phys. Rev. B **50**, 17271 (1994).
[7] J. Weis *et al.*, Phys. Rev. Lett. **71**, 4019 (1993).
[8] O. Agam *et al.*, Phys. Rev. Lett. **78**, 1956 (1997).
[9] H. van Houten, C. W. J. Beenakker and A. A. M. Staring, in "*Single Charge Tunneling, Coulomb Blockade Phenomena in Nanostuctures*" ed. H. Grabert and M. H. Devoret, NATO ASI series B 294 (Plenum Press, New York, 1991), pp. 167-216.
[10] D. Weinmann *et al.*, Phys. Rev. Lett **74**, 984 (1995).
[11] M. Ciorga *et al.*, Phys. Rev. B **61**, R16315 (2000).
[12] S. Tarucha *et al.*, Phys. Rev. Lett. **77**, 3613 (1996).
[13] L. P. Kouwenhoven *et al.*, Science **278**, 1788 (1997).
[14] S. Tarucha *et al.*, Phys. Rev. Lett. **84**, 2485 (2000).

[15] If the pulse height is made larger so that $U(1,\frac{1}{2}) > U(2,1)$ at $V_G = V_h$, the tunneling transitions from $(1,\frac{1}{2})$ to either $(2,0)$ or $(2,1)$ occurs more or less equivalently, but this provides no net transient current.
[16] The peak position reflects the orbital characteristic of the corresponding two states, $(2,1)$ and $(3,\frac{1}{2})$ for peak b, and $(2,0)$ and $(3,\frac{1}{2})$ for the GS-GS tunneling peak appearing between $N = 2$ and 3. We confirmed that the spacing between these two peaks corresponds to Δ_2 over the magnetic field range investigated (0 to 4 T).
[17] B. L. Altshuler *et al.*, Phys. Rev. Lett. **78**, 2803 (1997).
[18] The current increases or decreases depending on the tunneling conditions. This is partly explained in Ref. [4].